Mon. Not. R. Astron. Soc. **000**, 1–7 (2001) Printed 30 January 2002 (MN LATEX style file v1.4)

On the r-mode spectrum of relativistic stars: Inclusion of the radiation reaction

Johannes Ruoff and Kostas D. Kokkotas
Department of Physics, Aristotle University of Thessaloniki, Thessaloniki 54006, Greece

Accepted ???? Month ??. Received 2001 Month ??; in original form 2001 Month ??

ABSTRACT

We consider both mode calculations and time evolutions of axial r-modes for relativistic uniformly rotating non-barotropic neutron stars, using the slow-rotation formalism, in which rotational corrections are considered up to linear order in the angular velocity Ω. We study various stellar models, such as uniform density models, polytropic models with different polytropic indices n, and some models based on realistic equations of state. For weakly relativistic uniform density models, and polytropes with small values of n, we can recover the growth times predicted from Newtonian theory when standard multipole formulae for the gravitational radiation are used. However, for more compact models, we find that relativistic linear perturbation theory predicts a weakening of the instability compared to the Newtonian results. When turning to polytropic equations of state, we find that for certain ranges of the polytropic index n, the r-mode disappears, and instead of a growth, the time evolutions show a rapid decay of the amplitude. This is clearly at variance with the Newtonian predictions. It is, however, fully consistent with our previous results obtained in the low-frequency approximation.

Key words: relativity – methods: numerical – stars: neutron – stars: oscillations – stars: rotation

1 INTRODUCTION

The r-mode instability, and the associated spin-down of rapidly rotating young neutron stars, has created considerable interest in the astrophysical community, particularly as this may be a detectable source of gravitational waves. However, it was soon realized that a lot of effects tend to work against the growth of the r-mode. Viscous damping, coupling to the crust, magnetic fields and differential rotation could severely reduce the importance of the instability, if not suppress it completely. Since there is a large number of papers published on this subject we refer the reader to two recent reviews (Andersson & Kokkotas, 2001; Friedman & Lockitch, 2001).

Most of the results have been obtained in a Newtonian context, with radiation effects incorporated through the standard multipole formulae. However, in a first step towards a fully relativistic treatment, it was first shown by Kojima (1997, 1998) that the Newtonian treatment might actually miss important relativistic effects, such as the frame dragging. Working in the low-frequency approximation, which actually neglects any gravitational radiation, he showed that instead of having a discrete r-mode frequency, the frame dragging, being a function of the stellar radius r, gives rise to a whole band of frequencies. The existence of this continuous spectrum was proven by Beyer & Kokkotas (1999) in a rigorous way. However, it is still possible to find mode solutions for uniform density stars, as has been shown by Lockitch, Andersson & Friedman (2001). In a previous paper (Ruoff & Kokkotas, 2001), which we refer to henceforth as paper I, we have corroborated these results both through explicit mode calculations and through the evolution of the time dependent equations. However, at the same time we have shown that certain polytropic models, and some stellar models based on realistic equations of state, do not allow the existence of physical r-modes. Although for $l = 2$, it was always possible to find a mathematically valid mode solution with its eigenfrequency lying inside the continuous band, the associated fluid velocity was diverging at some point inside the star. Therefore, we considered such solutions as being unphysical, and hence non-existent. This view was supported by the

explicit time evolution of the relevant equations, as the system did not show any tendency to oscillate with the "unphysical" frequency predicted by the mode calculation.

These results were obtained in the low-frequency approximation, which amounts to neglecting the radiative metric perturbations. In this paper, we consider the complete set of axial equations, which follow from expanding the Einstein equations up to first order in the rotation rate Ω. However, we do not include the coupling to the polar equations. As we shall show, the main results from paper I concerning the existence of the r-mode more or less directly carry over to the fully relativistic case. This means that even if one takes into account the radiative back-reaction, there are certain cases where, at least within the slow-rotation approximation, discrete purely axial r-modes cannot be found.

2 MATHEMATICAL FORMULATION

If we focus on purely axial perturbations, the perturbed metric can be written in the following form:

$$ds^2 = ds_0^2 + 2\sum_{l,m}\left(h_0^{lm}(t,r)dt + h_1^{lm}(t,r)dr\right)\left(-\frac{\partial_\phi Y_{lm}}{\sin\theta}d\theta + \sin\theta\partial_\theta Y_{lm}d\phi\right) , \tag{1}$$

where $Y_{lm} = Y_{lm}(\theta,\phi)$ denote the scalar spherical harmonics. The unperturbed metric ds_0^2 represents a non-rotating stellar model with a first order rotational correction ω (the frame dragging) in the $t\phi$-component:

$$ds_0^2 = -e^{2\nu}dt^2 + e^{2\lambda}dr^2 + r^2\left(d\theta^2 + \sin^2\theta d\phi^2\right) - 2\omega r^2\sin^2\theta dt d\phi . \tag{2}$$

The fluid is assumed to rotate with uniform angular velocity Ω. The axial component of the fluid velocity perturbation can be expanded as

$$4\pi(p+\epsilon)\left(\delta u^\theta, \delta u^\phi\right) = e^\nu\sum_{l,m}U^{lm}(t,r)\left(-\frac{\partial_\phi Y_{lm}}{\sin\theta}, \sin\theta\partial_\theta Y_{lm}\right) . \tag{3}$$

Einstein's field equations then reduce to three equations for the three variables h_0^{lm}, h_1^{lm} and U^{lm} (Kojima 1992).

To obtain a system of equations, which is suitable for the numerical time evolution, the most straightforward way is to use the ADM-formalism (Arnowitt, Deser & Misner 1962, Ruoff 2001). For the axial perturbations, the expansion of the metric variables V_4, and extrinsic curvature variables K_3 and K_6, has been given in paper I. We just restate the connection between those variables and the ones defined above:

$$h_0 = e^{\nu-\lambda}K_6 , \tag{4}$$

$$h_1 = e^{\lambda-\nu}V_4 , \tag{5}$$

$$U = 4\pi e^{-\lambda-\nu}(p+\epsilon)(u_3 - K_6) . \tag{6}$$

The evolution equations for the variables V_4, K_3, K_6 and u_3 are

$$\left(\frac{\partial}{\partial t} + \mathrm{i}m\omega\right)V_4 = e^{2\nu-2\lambda}\left[K_6' + \left(\nu' - \lambda' - \frac{2}{r}\right)K_6 - e^{2\lambda}K_3\right] , \tag{7}$$

$$\left(\frac{\partial}{\partial t} + \mathrm{i}m\omega\right)K_3 = \frac{l(l+1)-2}{r^2}V_4 + \frac{2\mathrm{i}m}{l(l+1)}\omega' e^{-2\lambda}K_6 , \tag{8}$$

$$\left(\frac{\partial}{\partial t} + \mathrm{i}m\omega\right)K_6 = V_4' - \frac{\mathrm{i}mr^2}{l(l+1)}\left[\omega' K_3 - 16\pi\varpi(p+\epsilon)u_3\right] , \tag{9}$$

$$\left(\frac{\partial}{\partial t} + \mathrm{i}m\Omega\right)u_3 = \frac{2\mathrm{i}m\varpi}{l(l+1)}(u_3 - K_6) , \tag{10}$$

with the abbreviation

$$\varpi = \Omega - \omega . \tag{11}$$

Furthermore, we have one momentum constraint:

$$16\pi(p+\epsilon)u_3 = K_3' + \frac{2}{r}K_3 - \frac{l(l+1)-2}{r^2}K_6 - \frac{2\mathrm{i}m\omega'}{l(l+1)}e^{-2\nu}V_4 . \tag{12}$$

We could use this constraint to replace u_3 in Eq. (9) and thus obtain a complete set of three equations. However, we prefer to use the above set of four equations and use the constraint to monitor the numerical evolution. Of course, we also need the constraint (9) to construct valid initial data. We evolve the above system using a two-step Lax-Wendroff scheme yielding second order convergence, which can be easily checked by monitoring the violation of the momentum constraint (12) for different spatial resolutions.

The above system of evolution equations describe both the w- and r-modes. In this paper, we would like to focus on the r-modes only, and so we will try to minimise the w-mode contribution by choosing appropriate initial data. In addition we will compare the evolution of the full system with the evolution of the equations in the low-frequency approximation.

In the low-frequency approximation, $V_4 = 0$, and the evolution system involves only the variables K_6 and u_3. As initial data, we chose an arbitrary function for u_3 and solved the elliptic equation (32) of paper I for $h_0 = e^{\nu-\mu}K_6$. For the full system, we can do exactly the same. We set $V_4(t=0) = 0$ and choose an arbitrary function for u_3. Next, we solve Eq. (32) of paper I for K_6 and finally compute the remaining variable K_3 from the momentum constraint (12).

The conversion of the evolution system (7) – (10) into a time independent form is straightforward. Assuming a harmonic time dependence $e^{-i\sigma t}$, we can deduce the following two ordinary differential equations:

$$V_4' = \frac{\mathrm{i}mr^2}{l(l+1)}\left(\omega' K_3 - 16\pi\varpi(p+\epsilon)u_3\right) - \mathrm{i}\,(\sigma - m\omega)\,K_6\,, \tag{13}$$

$$K_6' = e^{2\lambda}K_3 - \left(\nu' - \lambda' - \frac{2}{r}\right)K_6 - \mathrm{i}e^{2\lambda-2\nu}\,(\sigma - m\omega)\,V_4\,, \tag{14}$$

together with the two algebraic relations:

$$K_3 = \frac{\mathrm{i}}{\sigma - m\omega}\left(\frac{l(l+1)-2}{r^2}V_4 + \frac{2\mathrm{i}m\omega'}{l(l+1)}e^{-2\lambda}K_6\right)\,, \tag{15}$$

$$u_3 = \frac{2m\varpi}{2m\varpi + l(l+1)(\sigma - m\Omega)}K_6\,. \tag{16}$$

Eq. (16) is equivalent to Eq. (40) of Paper I and is singular if the denominator becomes zero, which can only happen if σ is real. For real sigma, the expression $\sigma - m\omega$ can also vanish, and Eq. (15) becomes ill defined. However, as σ is expected to be a complex frequency, both equations for K_3 and u_3 should remain regular. Still, these singular structures can pose difficulties for the numerical treatment when the imaginary part of σ becomes very small.

We should make a few more remarks on the above system. In principle we could transform it into a single second order ODE for the quantity V_4. However, this equation would be rather messy since the necessary algebra leads to many terms quadratic in Ω and ω. If, however, we neglect any terms quadratic or of higher power in Ω and ω, we can recover Eq. (42) of Kojima (1992) with the polar source terms $F_{l\pm1m}$ set to zero. This equation was later used by Andersson (1998) to compute the rotational corrections to the axial w-modes and the r-modes.

However, as we shall show, the values given by Andersson for the r-modes cannot be corroborated neither through the time evolution nor through mode calculation with the above set of equations. This is because the extra terms that are not included in his form of the equations are critical, at least for the study of the r-modes. To be more specific, a basic property of the r-modes is that their frequency σ is proportional to the rotation rate Ω. This implies that the coefficient of K_6 in Eq. (16) is not of order Ω but of order 1, i.e. u_3 and K_6 are of the same order. If one looks for an equation similar to Eq. (42) of Kojima (1992), which is second order in σ, it is clear that one has to retain all the $O(\Omega^2)$ terms if one wants to correctly compute the r-mode frequencies, because in this case, it is $\sigma^2 = O(\Omega^2)$. However, in Eqns. (42) of Kojima (1992) and (10) of Andersson (1998), the $O(\Omega^2)$ terms were discarded, hence these equations are not suitable for computing correct r-mode frequencies.

Therefore, we leave Eqs. (13) – (14) as they are, and solve them as a coupled first order system. To this end we follow the method of Andersson (1998) and integrate (13) and (14) using a complex valued r coordinate in the exterior spacetime. In the asymptotic exterior, the behaviour of the perturbation variables is given by

$$X \sim X_{\mathrm{out}}e^{i\sigma r_*} + X_{\mathrm{in}}e^{-i\sigma r_*}\,, \tag{17}$$

with r_* being the well-known tortoise coordinate. The quasi-normal modes are defined as purely outgoing solutions, i.e. solutions with $X_{\mathrm{in}} = 0$. For a complex-valued frequency σ, the amplitude of one of the terms in Eq.(17) will always diverge if the integration is performed along the real r-axis. However, this can be overcome by choosing the path of integration in the complex r-plane to be a straight line with the angle to the real r-axis given by arg(r) = -arg(σ). In a region far enough from the stellar surface, we then test our solution by computing the Wronskian with the pure outgoing solution $e^{i\sigma r_*}$. The vanishing of the Wronskian tells us that we have found a quasi-normal mode of the star. We have tested this method by computing the axial w-modes for non-rotating neutron star models, reproducing the values given by Kokkotas (1994) for uniform density models and other polytropic models.

3 NUMERICAL RESULTS

3.1 Uniform density models

In the Newtonian limit, one can estimate the growth time for the $l = m = 2$ r-modes of uniform density models as (Kokkotas & Stergioulas, 1999)

Table 1. The r-mode frequency f and its growth time τ obtained from mode calculations for uniform density models with a central density of $\epsilon_c = 10^{15}$ g/cm^3 and rotational parameter $\varepsilon = 0.5$. The last column contains the growth time τ_{PN} computed by formula (18).

M/R	$M\,[M_\odot]$	R [km]	p_c [dyn/cm^2]	Period [ms]	f[Hz]	τ[s]	τ_{PN}[s]
0.1	0.384	5.671	5.637×10^{34}	0.546	1830	150	139
0.2	1.086	8.019	1.530×10^{35}	0.524	1906	13	12
0.3	1.996	9.822	3.681×10^{35}	0.495	2022	3.3	3
0.4	3.072	11.342	1.454×10^{36}	0.449	2226	1.3	1.1

$$\tau_{PN} = 22 \left(\frac{1.4M_\odot}{M}\right) \left(\frac{10\text{ km}}{R}\right)^4 \left(\frac{P}{1\text{ ms}}\right)^6 \text{s} \,. \tag{18}$$

In general, the growth time is proportional to P^{2l+2}, whereas the oscillation period increases linearly with the rotation period P. Of course, formula (18) has been derived by applying the standard multipole formulae for the mass and current multipole moments obtained from Newtonian theory. It is clear that for very compact stars, there should be deviations due to higher order corrections. In Fig. 1, we show the growth times for four uniform density models with different values of the compactness $M/R = 0.1$, 0.2, 0.3 and 0.4. In a double-logarithmic plot, a power law is represented by a straight line. For the less relativistic stellar models with $M/R = 0.1$ and 0.2, the agreement of formula (18) with the results of our mode calculations for $l = 2$ is very good, and for higher values of l, we can recover the $2l + 2$ dependence of the exponent, in fact we find that

$$\tau_{PN} \sim (|m|\Omega)^{2l+2} \,. \tag{19}$$

For more relativistic models, however, we find a systematic deviation and the growth time rather goes with a power of $2l + 3$, for small values of P. For large values of P, we still have a $2l+2$ dependence, however, formula (18) tends to underestimate the growth times, i.e. the instability is not as strong as formula (18) suggests. This weakening of the instability for very compact stellar models might be linked to the formation of a potential well inside the star, which can trap the gravitational waves. This would make it more difficult for the mode to grow. Nevertheless, for uniform density models with a compactness in the range of realistic neutron star models, the agreement between relativistic linear perturbation theory and the results from the multipole formula is very good.

In addition to mode calculations, we also performed the explicit evolution of the time dependent equations. The results for the four different compactness ratios are shown in Fig. 2. To make the growth time accessible to the numerical evolution, we have chosen the rotation rate to be $\varepsilon = 2.0$ corresponding to values of $P \approx 0.2$ ms. This is significantly above the Kepler limit, which is given approximately by $\varepsilon = \Omega/\sqrt{M/R^3} \approx 0.7$. Above this rotation rate the star becomes unstable with respect to mass shedding. Of course, in this case, the slow-rotation approximation is not valid any more, but if implemented correctly, the mode calculation and the time evolution should always yield the same complex-valued frequencies for any given value of ε. In all four cases, it is clearly discernible that after a short initial time, an exponentially growing mode appears, which soon dominates the evolution. From the mode calculations we obtain the growth times given in Table 1. In the graphs of Fig. 2, we have indicated these growth times by straight lines, matching exactly the amplitudes of the growing modes.

3.2 Polytropic models

In paper I, we have shown that in the low-frequency approximation, not all the polytropic stellar models can admit physical r-mode solutions. Nevertheless, it was in most cases possible to find a mathematically valid eigensolution satisfying the imposed boundary condition. However, if the mode frequency σ lay inside the range of the continuous spectrum, the associated fluid velocity u_3 was diverging at some point inside the star. Moreover, the metric variable h_0 exhibited an infinite slope at this particular point. Based on these facts, we considered such solutions as being unphysical, and hence nonexistent. We we able to corroborate our point of view by explicitly evolving the time dependent equation, which showed that there was no sign of a mode at the frequency predicted by the mode calculation. A further indication came from the behaviour of the amplitude of the metric variable h_0. In those cases where a physical mode existed, the amplitude remained constant after a certain initial time, whereas in the other cases, the amplitude kept decaying.

Of course, the low-frequency approximation is quite restrictive, since it cuts off the gravitational radiation. This is the reason why the associated eigenvalue problem becomes singular, as the mode frequencies have to be real valued. With the inclusion of the gravitational radiation, each mode acquires a finite imaginary part, being positive for a damped mode and negative for a growing mode. The addition of an imaginary part (no matter how small) to the mode frequencies removes the singular structure of the equations. Hence, it has been argued that in considering the problem with the inclusion of the gravitational radiation effect, one should be able to find the r-modes, with the anticipated growth times derived from Newtonian theory.

We find that this does not prove to be the case. For uniform density models, the equations are *always* regular, i.e. both with

and without the radiative terms, and it is always possible to find a physical r-mode. However, all those stellar models which did not admit physical r-modes in the low-frequency approximation *still* do not do so when radiation reaction is included. In other words, the qualitative picture which has emerged from the low-frequency approximation does not change at all.

In Fig. 3, we show the time evolution of the same initial data for a sequence of polytropic stellar models with fixed compactness $M/R = 0.3$, fixed rotation parameter $\varepsilon = 1.0$, but varying polytropic index n, ranging from $n = 0$ to $n = 1$. For $n = 0$, 0.2 and 0.4, we find the expected exponential growth, in agreement with the values computed from explicit mode calculations. However, for the other values $n = 0.6$, 0.8 and 1.0, no growth is visible and instead the amplitude decays. This decay becomes stronger as n is increased.

In Fig. 4, we show the imaginary parts of the frequency for a sequence of polytropic models with the polytropic index n ranging from $n = 0.3$ to $n = 0.8$ in steps of 0.05. Both panels show the same data. In the right panel, however, the plot is on a logarithmic scale and for a larger range of ε. It should be noted that the Kepler limit is reached for $\varepsilon \approx 0.7$, hence any value of ε above is unphysical. We nevertheless show the behaviour of the growth times up to $\varepsilon = 2.5$, in order to gain more insight into how the mode disappears. For $n = 0.3$, the growth times follows the expected power law in the range from $\varepsilon = 0.1$ to $\varepsilon \approx 1.5$. For larger ε, a deviation becomes obvious. As n is increased, this deviation becomes more pronounced and a bulge starts to emerge at $\varepsilon \approx 1.8$, at which the imaginary parts tend to become smaller. Recall that smaller imaginary part means longer growth time. For $n = 0.5$, the curve exhibits a local minimum at $\varepsilon \approx 1.8$. For $n \geq 0.55$ the curves cross the zero line at some specific value of ε and reappear at some larger value of ε. The larger n is, the sooner the imaginary part becomes zero, and the larger ε is at the reappearance point. For $n = 0.8$, the imaginary part becomes zero at $\varepsilon \approx 0.6$, for larger n this occurs even for much smaller ε.

From the left panel of Fig. 4, one could be led to the conclusion that the imaginary part does not vanish but actually crosses the ε-axis and becomes negative. This would correspond to the r-mode being damped. However, this seems not to be the case. What happens instead is that it becomes impossible to numerically find the mode at all. Of course, numerically not finding the mode does not mean that the mode ceases to exist for certain parameters, but from the analogy with the results of the low-frequency approximation, we conclude that the r-mode does indeed vanish, and there is only the (non-radiative) continuous spectrum left. This view is corroborated by the numerical evolutions, which in those cases show the decay of the metric amplitude, whereas each fluid layer oscillates with its own frequency, keeping a constant amplitude in exactly the same way as it did in the low-frequency approximation. This is clarified in Fig. 5, where we show the evolution of the same initial data, once using the full set of equations, and once using the low-frequency approximation. We plot the amplitudes of both the fluid variable u_3 (somewhere inside the star) and the metric variable K_6 (somewhere outside the star). As it can been seen, after about 10 ms, the fluid variable u_3 remains at the same constant amplitude for both cases, whereas K_6 keeps decaying. It decays even faster in the full case than in the low-frequency approximation. The amplitude of K_6 is smaller from the very beginning because the radiative metric variable V_4 absorbs some of the energy of the initial data and radiates it away in a sharp pulse. This is not possible in the low-frequency approximation, since there the radiation effects are neglected.

Finally, in Fig. 6, we show the dependence of the complex mode frequency σ on the polytropic index n, for a sequence of polytropic models with fixed compactness $M/R = 0.2$ and a rotation period of 1.0 ms. We plot both the real and the imaginary part of σ in the same graph, using the left scale for the real part and the right scale for the imaginary part. In addition we include the region of the continuous spectrum, which is bounded by

$$m\Omega\left(1 - \frac{2\varpi(0)}{\Omega l(l+1)}\right) < \sigma_{cont} < m\Omega\left(1 - \frac{2\varpi(R)}{\Omega l(l+1)}\right) \ . \tag{20}$$

For small n, the real part $\mathrm{Re}(\sigma)$ lies outside the range of the continuous spectrum, but for increasing n it approaches the lower boundary. The imaginary part $\mathrm{Im}(\sigma)$ first grows with increasing n, but eventually turns around and drops sharply down to zero. In this case, $\mathrm{Re}(\sigma)$ reaches the lower boundary of the continuous spectrum and $\mathrm{Im}(\sigma)$ goes to zero for $n = 0.843$. No mode can be found for larger n.

3.3 Realistic models

As with the polytropic models, we can more or less take over the results of paper I for models which are based on a realistic EOS. It is for the stiffest EOS that r-modes can exist for the whole physically acceptable mass range, whereas for intermediate EOS, the r-mode vanishes if the compactness exceeds a certain critical value. For the softest EOS, none of the models can support r-modes.

4 SUMMARY

We have performed both mode calculations and time evolutions of purely axial perturbations of rotating neutron stars using the slow-rotation approximation, i.e. including only rotational correction terms linear in the angular velocity Ω. This work

is thus an extension of our previous results of Paper I. We have shown that on the one hand, we are in full agreement with Newtonian-limit predictions for uniform density models, but on the other hand, we obtain completely different results for relativistic stars obeying polytropic equations of state with the polytropic index n being larger than about 0.8. In agreement with our previous analysis of the r-modes in the low-frequency approximation (Paper I), we showed that in these cases, no discrete r-modes can be found.

For the uniform density models, we find that for less relativistic models, the growth time is well described by a power law with an exponent of $2l+2$, whereas for more relativistic models the strength of the instability is somewhat suppressed. We conjecture that this can be traced back to the appearance of a potential well inside the star, which on the one hand can trap the gravitational waves and thus give rise to very long-lived spacetime modes (the trapped modes), but on the other hand should reduce the growth of the unstable r-mode.

In Paper I, we have shown that due to the singular structure of the eigenvalue equation in the low-frequency approximation, there exists a class of physically reasonable stellar models based on polytropic or certain soft realistic equations of state, which does not permit the existence of physical r-modes. As a result of the present work, it became clear that even with the inclusion of the gravitational radiation reaction, the slow-rotation approximation can still fail to yield the r-mode solutions expected from Newtonian theory. Although we can find very good agreement for uniform density models, the r-modes seem to disappear for the relativistic polytropic cases with large polytropic index n.

It might well be that inclusion of higher order corrections in Ω or the coupling to the polar equations will drastically change the above picture, and relativistic r-modes can be found for any stellar model. However, it also might be the case that the above picture persists, and that the r-modes simply do not exist for certain stellar models, which might be a consequence of the relativistic frame dragging. A first hint in this direction might come from recent results by Karino et al. (2001). They computed the r-modes of rapidly and differentially rotating Newtonian polytropic models without resorting to the slow-rotation approximation. They found that for certain parameters of the rotation, their numerical scheme ceases to yield mode solutions, because of the appearance of co-rotation points. Through this analogy, we may conjecture that the same could hold in the rapidly rotating case, where one does not expand the equations in terms of Ω. Of course, not finding the modes numerically does not prove their non-existence. However, the results of Karino et al. (2000) seem at least to indicate that even if there exist r-modes in the regime where their code failed to detect any, they might at least be strongly affected by the differential rotation and have quite different physical properties than the r-modes in weakly differentially or uniformly rotating stars.

The same could be true for the relativistic r-modes of those stellar models where, within the slow-rotation approximation, one cannot find any, as the relativistic frame dragging has an effect similar to that of differential rotation. If it is only by including higher order terms that the true physical r-modes can be found, we might expect them to have quite different physical properties, and probably much larger growth times, as would be expected from Newtonian theory. Of course, if the true EOS of a neutron star is such that it already permits the existence of r-modes in the slow-rotation approximation, i.e. if the EOS is rather stiff, and unless other physical mechanism do not prevent the r-mode from growing, then the results obtained from Newtonian theory should be reliable. On the other hand if the EOS is rather soft, then it might well turn out that the implications of the r-mode instability, as based on Newtonian estimates, such as spin-down scenarios and gravitational wave emission, might be less significant. Either way, a full understanding of the relativistic r-modes is still outstanding and has to take into account at least the coupling to the polar equations, if not even the inclusion of all Ω^2 corrections.

ACKNOWLEDGEMENTS

We thank Nils Andersson, Horst Beyer, John Friedman, Ian Jones, Luciano Rezzolla, Bernard F. Schutz, Adamantios Stavridis, Nikolaos Stergioulas and Shin Yoshida for helpful discussions. J.R. is supported by the Marie Curie Fellowship No. HPMF-CT-1999-00364. This work has been supported by the EU Programme 'Improving the Human Research Potential and the Socio-Economic Knowledge Base' (Research Training Network Contract HPRN-CT-2000-00137).

REFERENCES

Andersson N., 1998, ApJ, 502, 708
Andersson N., Kokkotas K.D., 2001, Int. J. Mod. Phys. D, in press; gr-qc/0010102
Arnowitt R., Deser S., Misner C.W., 1962, in Witten L., ed., Gravitation: An Introduction to Current Research. Wiley, New York, p.227
Beyer H.R., Kokkotas K.D., 1999, MNRAS, 308, 745
Friedman J.L., Lockitch K.H., 2001, gr-qc/0102114
Karino S., Yoshida S., Eriguchi Y., 2001, Phys. Rev. D, 64, 024003
Kojima Y., 1992, Phys. Rev. D, 46, 4289
Kojima Y., 1997, Prog. Theor. Phys. Suppl., 128, 251
Kojima Y., 1998, MNRAS, 293, 49

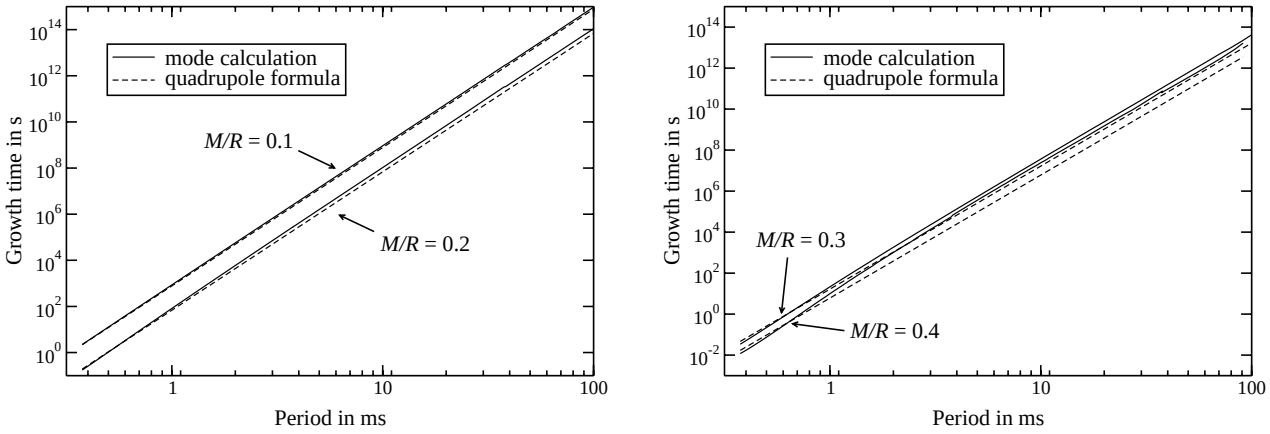

Figure 1. Double logarithmic plot of the growth time for uniform density models with compactness $M/R = 0.1$, 0.2 (left panel) and $M/R = 0.3$, 0.4 (right panel). Also included is the growth time deduced from formula (18). For $M/R = 0.1$ and 0.2, the agreement very good, whereas for $M/R = 0.3$ and in particular for $M/R = 0.4$, there is a systematic deviation, and formula (18) tends to overestimate the growth rate.

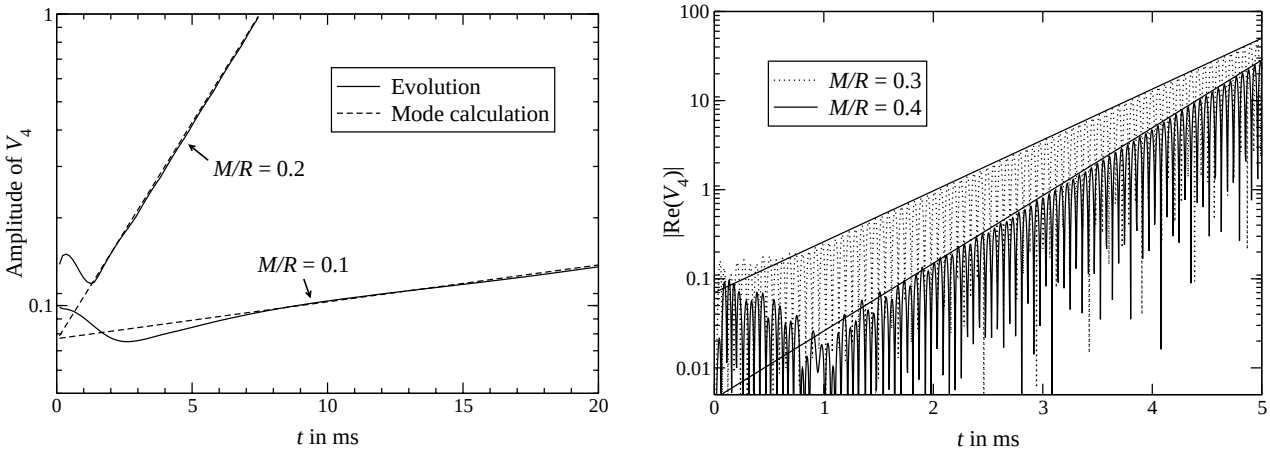

Figure 2. Evolution of the 4 uniform density models of Table 1. Each model permits the existence of an r-mode, and the evolution shows the expected exponential growth in the amplitude. Also included are the slopes of the growth obtained from mode calculations. In the right panel, we have plotted only the amplitude of V_4 since the oscillations would be too dense.

Kokkotas K.D., 1994, MNRAS, 268, 1015; Erratum: 1995, 277, 1599
Kokkotas K.D., Stergioulas N., 1999, A&A , 341, 110
Lockitch K.H., Andersson N., Friedman J.L., 2001, Phys. Rev. D, 63, 024019
Ruoff J., 2001, Phys. Rev. D, 63, 064018
Ruoff J., Kokkotas K.D., 2001, gr-qc/0101105

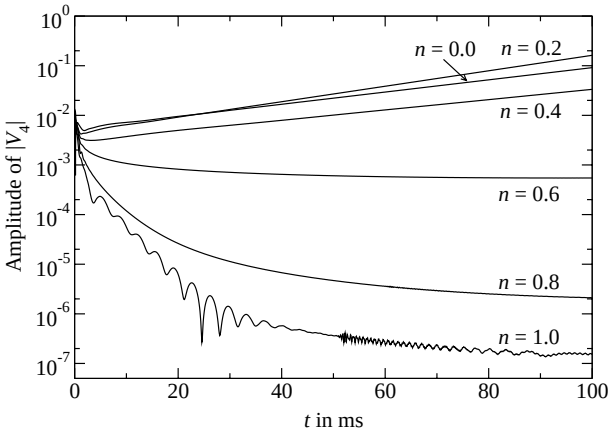

Figure 3. Amplitude of V_4 for polytropic stellar models with the same compactness $M/R = 0.3$ and rotational parameter $\varepsilon = 1.0$, but differing values of the polytropic index n, ranging from $n = 0$ to $n = 1$. For $n = 0$, 0.2 and 0.4, the evolutions show exponential growth, whereas for values of $n \geq 0.6$, the amplitudes decay.

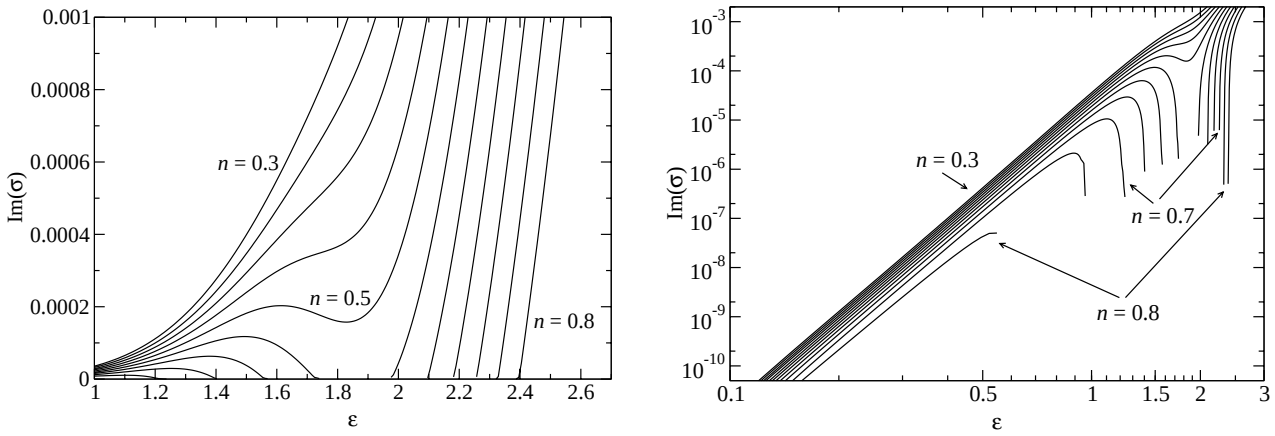

Figure 4. Growth times of the r-mode as a function of the rotational parameter ε for a sequence of polytropic stellar models with the polytropic index n ranging from $n = 0.3$ to $n = 0.8$ in steps of 0.05. As n is increased a deviation from the power law starts to emerge. Note that the values $\varepsilon > 0.7$ are unphysical and are included only to gain a better understanding of the behaviour of the growth times for $\varepsilon < 0.7$.

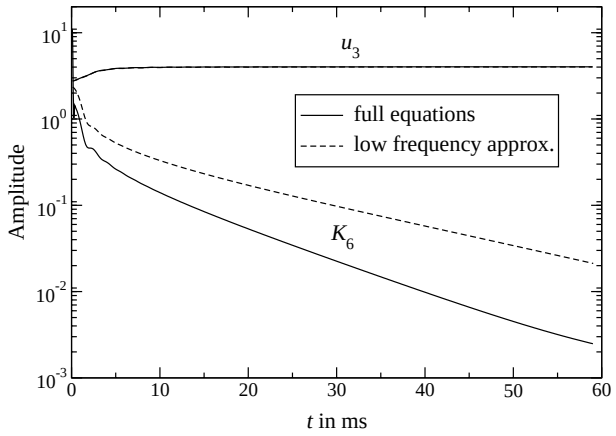

Figure 5. Comparison of the evolution of the same initial data in the full case and in the low-frequency approximation for a stellar model which does not possess a physical r-mode. It is shown the amplitude of K_6 outside the star together with the velocity perturbations u_3 extracted in the middle of the star. In both cases the fluid perturbation are almost identical and cannot be distinguished in the graph. Furthermore, for the full equations, the decay of K_6 is even stronger than in the low-frequency approximation.

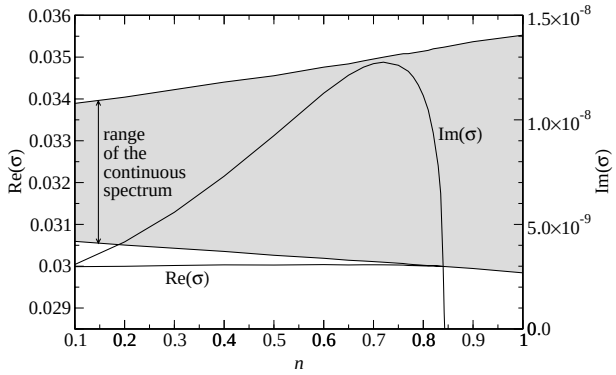

Figure 6. Behaviour of the real and imaginary part of the r-mode frequency σ as a function of the polytropic index n for models with $M/R = 0.2$ and rotation period of 1.0 ms. The scale on the left is for the real part, the scale on the right for the imaginary part of σ. For small n, the real part $\mathrm{Re}(\sigma)$ lies outside the range of the continuous spectrum. For increasing n, $\mathrm{Re}(\sigma)$ approaches the lower boundary and the imaginary part $\mathrm{Im}(\sigma)$ eventually starts to decrease. For $n = 0.843$, $\Re(\sigma)$ reaches the lower boundary of the continuous spectrum and $\mathrm{Im}(\sigma)$ goes to zero. For larger n, no mode can be found any more.